

## Studies of pilocarpine:carbomer intermolecular interactions

Ariana Zoppi<sup>a</sup>, Yamila Garro Linck<sup>b</sup>, Gustavo A. Monti<sup>b</sup>, Diego B. Genovese<sup>c</sup>,  
Álvaro F. Jimenez Kairuz<sup>a</sup>, Rubén H. Manzo<sup>a</sup>, Marcela R. Longhi<sup>a,\*</sup>

<sup>a</sup> Departamento de Farmacia, Facultad de Ciencias Químicas, Universidad Nacional de Córdoba, Ciudad Universitaria, 5000 Córdoba, Argentina

<sup>b</sup> Facultad de Matemática, Astronomía y Física and IFEG (CONICET), Universidad Nacional de Córdoba, Córdoba, Argentina

<sup>c</sup> Laboratorio de Alimentos Instituto PLAPIQUI (UNS-CONICET), Camino La Carrindanga Km 7, CC 717, B8000FWB Bahía Blanca, Buenos Aires, Argentina

### ARTICLE INFO

#### Article history:

Received 24 June 2011

Received in revised form 31 January 2012

Accepted 5 February 2012

Available online 13 February 2012

#### Keywords:

Pilocarpine

Carbomer

Drug stability

NMR spectroscopy

Thermal analysis

Fourier-transform infrared spectroscopy

### ABSTRACT

The interactions between pilocarpine (PIL) and the anionic polyelectrolyte carbomer (CBR) were investigated. The effects of the chemical interactions on the chemical stability of the drug also were evaluated. The binary system was characterized by nuclear magnetic resonance techniques, Fourier-transform infrared spectroscopy (FT-IR), X-ray powder diffraction, scanning electron microscopy (SEM) and thermal analysis. The experiments showed that the complex, prepared by freeze-drying, is a solid amorphous form different from its precursors, thereby offering an interesting alternative for the preparation of extended release matrices. The solution stability of PIL was studied at pH 7 and 8, at 70 °C. The PIL solution stability was evaluated alone and in the presence of CBR. Results indicated that the drug in the presence of the polymer is 3.3 and 3.5 times more stable, at pH 7 and pH 8, respectively, than the drug without CBR. The activation energy and the frequency factor, according to Arrhenius plot, were estimated to be  $13.9 \pm 0.4$  and  $14.8 \pm 0.5 \text{ kcal mol}^{-1}$ , and  $6.1 \pm 0.3$  and  $7.6 \pm 0.3$ , with and without the polymer, respectively.

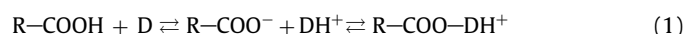
© 2012 Elsevier B.V. All rights reserved.

## 1. Introduction

Pilocarpine (PIL, Fig. 1a) is a cholinergic agonist used in eye drops for the treatment of open-angle and other chronic glaucomas. It is used in hydrochloride or the nitrate form, usually as 0.5–4% eye drops given up to 4 times daily (Sweetman and Blake, 2009). In addition, pilocarpine hydrochloride oral solid dosage forms are used to treat the xerostomia associated with Sjögren's syndrome and in radiotherapy for malignant neoplasms of head and neck. For the treatment of these pathologies is usually taken 3–4 times a day (Sweetman and Blake, 2009; Clinical Pharmacology Online, 2009).

A problem with the ocular administration of PIL in aqueous eye drops is that the aqueous solution of PIL is subjected to chemical degradation. To obtain an optimal stability, the eye drops are formulated at pH between 4 and 5, despite the drug being almost ionized at these values, which can reduce its ocular absorption (Connors et al., 1986; Jarvinen et al., 1994). Related to this, the main reactions that contribute to its instability are the hydrolysis of the  $\gamma$ -lactone moiety, producing pilocarpic acid and epimerization at the  $\alpha$ -carbon of the lactone ring, resulting in the formation of isopilocarpine; which can then degrade by hydrolysis to isopilocarpic acid (Fig. 1b and c) (Bundgaard and Hansen, 1982; Al-Badr and Aboul-Enein, 1983).

It is known that the complex formation between drugs and some excipients often leads to the stabilization of the active principles involved, with the forces including van der Waals forces, dipole–dipole interactions, hydrogen bonding, Coulomb forces and hydrophobic interactions (Yoshioka and Stella, 2002). An example of this kind of excipient is Carbomer (CBR, Fig. 1e), an anionic mucoadhesive polymer widely employed in ophthalmic formulations. CBR has protonable carboxylic groups linked to the molecular network of the polyelectrolyte, which allow interactions with oppositely charged drugs through the formation of a polyelectrolyte-drug complex, given by Eq. (1):



where R-COO<sup>−</sup> and R-COO<sup>−</sup> are the carboxylic and carboxylate groups of CBR, D and DH<sup>+</sup> are the neutral and protonated drug species.

In aqueous dispersions, the ionic-pair formation yields a high proportion of counterionic condensation with numerous different basic drugs, exhibiting both high affinity constants and negative electrokinetic potential (Jimenez-Kairuz et al., 2002; Vilches et al., 2002). These properties are relevant for different pharmaceutical applications, such as: modified-controlled drug delivery (Jimenez-Kairuz et al., 2003, 2005) and compatibility increase of low soluble drugs (Vilches et al., 2002). Additionally, it has been reported that the interaction of CBR with the basic drugs procaine (Jimenez-Kairuz et al., 2002) and azithromycin (Esteban et al., 2009) enhances their chemical stability in aqueous solutions.

\* Corresponding author. Tel.: +54 351 433 4163x107; fax: +54 351 433 4163x115.

E-mail address: mrlcor@fcq.unc.edu.ar (M.R. Longhi).

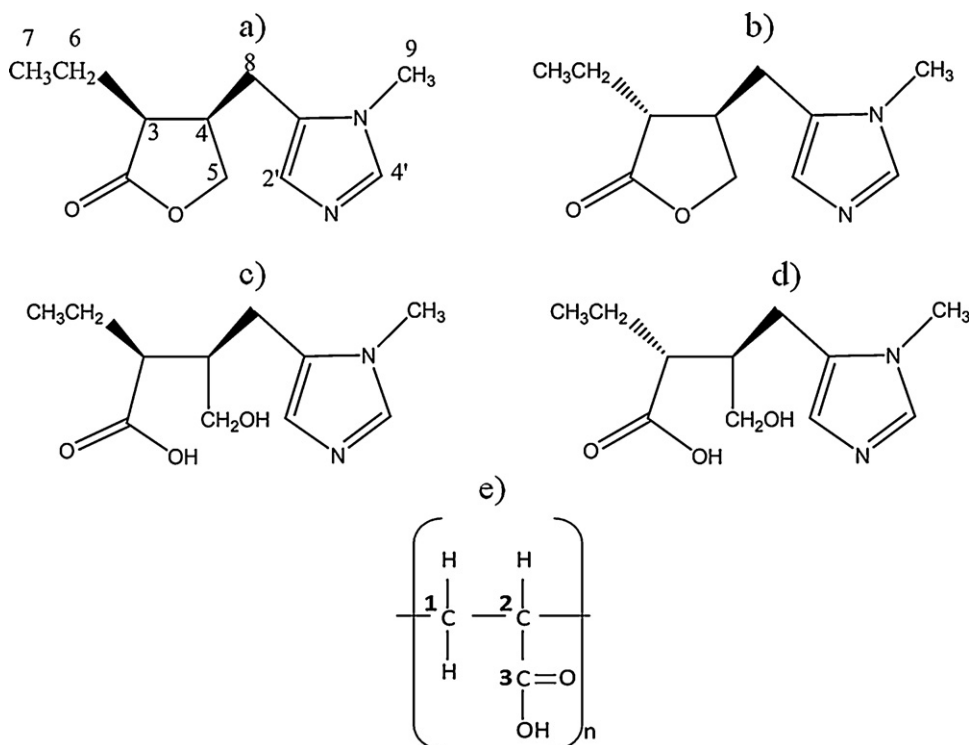


**Fig. 1.** Molecular structure of (a) pilocarpine, (b) isopilocarpine, (c) pilocarpic acid, (d) isopilocarpic acid and (e) carbomer.

In this work, we decided to study the interaction between PIL and CBR, in order to evaluate the influence of complexation on drug stability. Due to the short biological life of PIL (Clinical Pharmacology Online, 2009), the dosage regimen of PO tablets requires several daily doses. Therefore, it was considered of interest to obtain PIL:CBR complexes in solid state, since they can be used to prepare extended release matrices.

Nuclear magnetic resonance (NMR) techniques and high performance liquid chromatography (HPLC) were used to determine, the PIL:CBR interactions in aqueous medium and the chemical stability of the complex, respectively. In addition, PIL:CBR interactions were studied in the solid state by Fourier-transform infrared spectroscopy (FT-IR), solid state NMR (SSNMR), X-ray powder diffraction, scanning electron microscopy (SEM) and thermal analysis [differential scanning calorimetry (DSC) and thermogravimetric analysis (TGA)].

## 2. Materials and methods

### 2.1. Materials

Pilocarpine hydrochloride was a gift from Laboratorios Beta (Argentina). The pilocarpine base was obtained by extractions with chloroform from water solutions of pH 10.0.  $D_2O$  99.9 at.% D for NMR experiments (Sigma-Aldrich®). All other materials and solvents were of analytical reagent grade. A Milli-Q Water Purification System (Millipore®, Bedford, Massachusetts, USA) generated the water used in these studies. In addition,  $H_3BO_3/Na_2B_4O_7$  0.1 M buffers (pHs 7.0 and 8.0) were used (pH-meter HI 255, HANNA Instrument, Romania), with their ionic strength being adjusted to 0.5 by the addition of NaCl.

### 2.2. Preparation of PIL:CBR hydrogels

PIL:CBR hydrogel was prepared by neutralizing 0.1% aqueous dispersion of CBR with the appropriate amount of PIL base required

to neutralize 100% of the acidic groups of CBR. This dispersion was then stirred at 25 rpm for 3 h, using a magnetic stirring bar at room temperature. The pH of the hydrogel was measured, and adjusted by the addition of NaOH to pH 7.0 or 8.0, when necessary.

### 2.3. Preparation of the PIL:CBR complex in solid state

Hydrogel of CBR at 0.1% (w/w) was prepared in the form indicated in Section 2.2, and then frozen at  $-40^{\circ}C$  before being freeze-dried (Freeze Dry 4.5 Labconco Corp., Kansas City, MI).

### 2.4. Solution NMR Studies

All solution NMR experiments were performed on a Bruker® Avance II High Resolution Spectrometer, equipped with a Broad Band Inverse probe (BBI) and a Variable Temperature Unit (VTU). The spectra were measured at 298 K, adjusting the samples to pH 7. Operating frequency for protons was 400.16 MHz. Chemical shift of the residual solvent at 4.8 ppm used as an internal reference. The induced changes in the  $^1H$  chemical shifts for PIL ( $\Delta\delta$ ), which originated due to its complexation were, calculated using the following equation, Eq. (2):

$$\Delta\delta = \delta_{\text{complex}} - \delta_{\text{free}} \quad (2)$$

### 2.5. Stability studies

The chemical stability of PIL with or without CBR was studied as a function of temperature ( $40^{\circ}C$ ,  $50^{\circ}C$ ,  $60^{\circ}C$  and  $70^{\circ}C$ ) at two pH values (7.0 and 8.0). The hydrogels for these studies were prepared in the form indicated in Section 2.2, and free PIL was prepared in borate buffer solutions of pH 7.0 or 8.0. The samples were then placed in a thermostatic water bath (Circulators HAAKE F3-K, Germany), and were removed at various time intervals.

The determination of PIL was carried out by applying the HPLC method reported by Wong et al. (Wong et al., 1991), with modifications and was fully validated according to the ICH guideline

Q2 (R1) (International Conference on Harmonization, 2005). In order to identify the degradation products, to establish the intrinsic stability of the molecule and to validate the stability indicating power of the analytical procedure used, the stability stress testing for PIL was done in accordance with the ICH guideline Q1A(R2) (International Conference on Harmonization, 2003). The HPLC equipment consisted of an Agilent S1100 system, with a Hypersil ODS (4.6 × 250 mm, 5 µm, Thermo Electron Corporation, USA) reversed-phase column being used for separation. The mobile phase was a methanol:pH 7.7 potassium phosphate buffer (50 mM) 20:80 mixture, at a flow rate of 1.3 ml/min. Assays were performed at 45 °C, by injecting 10 µl of solution for each chromatographic run. The retention times for pilocarpic acid, isopilocarpic acid, isopilocarpine and PIL were 3.1 min, 4.1 min, 11 min and 12.2 min, respectively.

The observed first-order rate constants for degradation of free PIL [ $k_{\text{obs}(\text{free})}$ ] and PIL complexed with CBR [ $k_{\text{obs}(\text{complex})}$ ] were determined by applying a linear regression analysis of the plots of the natural logarithm of the remaining PIL concentration versus time. The values of  $E_a$ , and  $\log A$  for PIL, with or without CBR, were calculated from the Arrhenius plot.

## 2.6. Zeta potential measurement

The zeta potential of the hydrogel was measured by using a Malvern Zetasizer 3000 (Malvern Instruments Inc., London, UK), the temperature of the samples was controlled at 25 °C. The hydrogel (pH 7.0) was diluted to obtain the appropriate concentrations prior to measurement.

## 2.7. Fourier transform infrared spectroscopy

The FT-IR spectra of PIL, CBR and PIL:CBR complex were measured as potassium bromide discs on a Nicolet 5 SXC FT-IR Spectrometer, with the FT-IR spectrum of the PIL:CBR complex being compared with the PIL and CBR ones. All spectra were obtained and processed using EZ OMNIC E.S.P v.5.1 software.

## 2.8. Solid state nuclear magnetic resonance studies

The high resolution solid state  $^{13}\text{C}$  cross polarization/magic angle spinning (CP/MAS) spectra for pure components (PILHC and CBR) and the PIL:CBR complex were recorded using a ramp CP/MAS sequence with proton decoupling during acquisition. All solid state NMR experiments were performed at room temperature using a Bruker Avance II spectrometer operating at 300.13 MHz for proton and equipped with a 4 mm MAS probe. The operating frequency for carbons was 75.46 MHz. Adamantane was used as an external reference for the  $^{13}\text{C}$  spectra and for setting the Harmann–Hahn matching condition in the cross-polarization experiments with the spinning rate being 10 kHz. For all the samples, 2024 scans were recorded in order to obtain an adequate signal to noise ratio. The recycling time was 5 s and the contact time during CP was 2 ms. A two-pulse phase modulation (TPPM) sequence was used for decoupling during acquisition, with a proton field  $H_{1\text{H}}$  satisfying  $\omega_{1\text{H}}/2\pi = \gamma_{\text{H}}H_{1\text{H}}/2\pi = 60$  kHz (Bennet et al., 1995). Quaternary carbon edition spectra were recorded for all the samples. These spectra were acquired with the non-quaternary suppression (NQS) sequence, where the  $^1\text{H}$  and  $^{13}\text{C}$  radiofrequency fields are removed during 40 µs after CP and before the acquisition. This delay allows the carbon magnetization to decay because of the  $^1\text{H}$ – $^{13}\text{C}$  dipolar coupling, which results in spectra where CH and CH<sub>2</sub> are substantially removed (Harris, 1994).

**Table 1**  
Proton NMR chemical shifts of PIL, in the free and complex form.

Protons of PIL	$\delta_{\text{free}} \text{ PIL (ppm)}$	$\delta_{\text{complex}} \text{ PIL:CBR (ppm)}$	$\Delta\delta^a$ (ppm)
H7	1.0763	1.0793	0.0030
H6	1.7389	1.7328	-0.0061
H8	2.6982	2.7844	0.0862
H3	2.9196	2.9440	0.0244
H4	3.0650	3.1309	0.0659
H9	3.6446	3.8050	0.1604
H5	4.2869	4.3067	0.0198
H4'	6.8668	7.2490	0.3822
H2'	7.6659	8.4916	0.8257

<sup>a</sup>  $\Delta\delta = \delta_{\text{complex}} - \delta_{\text{free}}$ .

## 2.9. X-ray powder diffraction studies

The X-ray powder diffraction patterns were recorded on a Rigaku Miniflex 2000 X-ray diffractometer, using Ni-filtered Cu-K $\alpha$  radiation at 30 kW 15 mA and a scan rate of 0.05°/min. The diffractograms were recorded from 5° to 40° (2 $\theta$ ), and data were obtained using Standard Measurement software.

## 2.10. Scanning electron microscopy studies

Microscopic morphological structures of the raw materials and the complex were investigated and photographed using a scanning electron microscope LEO Model EVO 40XVP. The samples were fixed on a brass stub using double-sided aluminum tape and then made electrically conductive by employing a sputter coater PELCO Model 3 to perform gold coating in a vacuum. The magnification selected was sufficient for observing in detail the general morphology of the samples under study.

## 2.11. Differential scanning calorimetry and thermogravimetric analysis

Differential scanning calorimetry measurement of the pure materials and binary systems was carried out using a DSC TA 2920 (TA Instruments, Inc., New Castle, USA), and the thermal behavior was studied by heating 1–3 mg of samples in a sealed aluminum pan, from 25 to 350 °C at a rate of 10 °C min<sup>-1</sup> under nitrogen gas flow. A sealed empty pan was used as reference, and indium (99.98%, mp 156.65 °C, Aldrich, Milwaube, USA) as the standard for calibrating the temperature.

The TGA curves of the different samples were recorded on a TG TA 2950 (TA Instruments, Inc., New Castle, USA), using the same conditions as in the DSC studies. TG temperature axes were calibrated with the Curie point of Ni (353 °C). In both cases, data were obtained and processed using TA Instruments Universal Analysis 2000 software.

## 3. Results and discussion

### 3.1. PIL:CBR complex structure elucidation

#### 3.1.1. $^1\text{H}$ NMR studies

In order to study the structure of the PIL:CBR complex, the spectrum of pure PIL was compared to its corresponding signals in the complex. In Table 1 the chemical shifts of all the PIL protons in the free and complex form are summarized (see proton numbering in Fig. 1a). It can be observed that in the presence of the poly-electrolyte, almost all the protons resonances of PIL experienced shifts to higher ppm. Moreover, it is important to note that the protons H9, H2' and H4' of PIL are those which show the major displacements with respect to those of the pure drug. This behavior

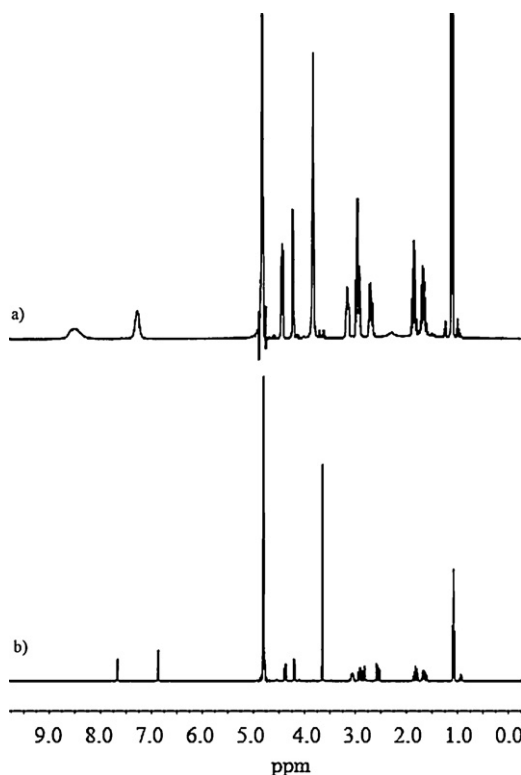


Fig. 2.  $^1\text{H}$  NMR spectra of complex (a) and PIL in free (b) form.

indicates that the PIL aromatic ring containing the protonable group of the molecule suffer the main disturbance after the complex formation. These observations indicate that complexation takes place through electrostatic interactions between the basic group of PIL and the acid group of CBR.

The shifts of the resonances to higher frequencies observed for the protons mentioned above are due to the deshielding effect produced by the proximity of the negatively charged carboxylic groups of CBR. In addition, it is necessary to emphasize that H9, H2' and H4' show broader peaks in the spectrum of the complex than in the free drug (Fig. 2), this behavior is probably associated to a decrease in the mobility of this moiety of the drug, caused by the complex formation with CBR. The changes observed in the chemical shifts of the other PIL protons may arise as a direct consequence of a binding interaction with the macromolecule, or indirectly as a result of a conformational change associated with the complexation.

### 3.1.2. DOSY studies

Based on the considerable difference in molecular sizes between PIL and CBR, we decided to conduct the DOSY experiments were carried out in order to determine how the diffusion coefficient ( $D$ ) of the drug is modified by the presence of CBR. The diffusion coefficient represents the ease of movement of a particular solute in a given solvent and is characteristic of both the solute and the solvent medium. The diffusion behavior of the drug depends on intrinsic characteristics of the molecule, such as size, shape, mass and charge, as well as on the surrounding environment (e.g. presence of other components in the solution, temperature, ability to form complexes or self-aggregation and viscosity of the medium) (Huo et al., 2003).

DOSY experiments were performed at constant room temperature (298 K) and pH 7. In order to establish if there was any change in  $D$  due to the viscosity of the hydrogel, four systems of varying CBR concentrations were tested, keeping the degree of neutralization of the acid groups of the polymer constant (100%).

**Table 2**  
Diffusion coefficient of PIL in the free and complex form.

Sample	$D$ ( $\text{m}^2/\text{s} \times 10^{10}$ )
PIL free	$7.50 \pm 0.03$
PIL:CBR 0.1%	$4.20 \pm 0.03$
PIL:CBR 0.08%	$4.21 \pm 0.03$
PIL:CBR 0.067%	$4.20 \pm 0.03$
PIL:CBR 0.05%	$4.23 \pm 0.03$

**Table 3**  
Values of  $k_{\text{obs}}$ ,  $t_{1/2}$  and  $t_{90}$  at 70 °C of PIL in the free and complex form.

System	pH	$k$ ( $\text{h}^{-1} \times 10^2$ )	$t_{1/2}$ (h)	$t_{90}$ (h)
PIL free	7.00	$2.02 \pm 0.08$	$34 \pm 1$	$5.2 \pm 0.2$
	8.00	$7.04 \pm 0.03$	$9.9 \pm 0.4$	$1.49 \pm 0.07$
Complex PIL:CBR	7.00	$0.61 \pm 0.08$	$114 \pm 14$	$17 \pm 2$
	8.00	$2.01 \pm 0.03$	$34.5 \pm 0.5$	$5.22 \pm 0.08$

Experimental results (Table 2) show a significant decrease in the diffusion coefficient of the drug in the presence of the polyelectrolyte. In addition, to the low concentrations of polyelectrolyte utilized in this study, it was observed that the viscosity did not present a predominant role, since the decrease in the concentration of CBR did not lead to an increase of the  $D$  value for PIL. Therefore, these observations confirm that the decrease in the  $D$  value of the drug is mainly due to the PIL interaction with CBR, which brought about a change in the hydrodynamic radius of the drug.

### 3.2. Stability studies

Comparative kinetic runs of PIL, with and without CBR, were performed at two-selected pHs (7.0 and 8.0) at 70 °C, and the determination of PIL and its degradation products was carried out by HPLC. In all systems studied, the main degradation products of PIL were isopilocarpine, pilocarpic acid and isopilocarpic acid, with the degradation process following a pseudo first-order kinetic. From the kinetic process, it was possible to calculate the apparent first degradation rate constant, half-life ( $t_{1/2}$ ) and  $t_{90}$ , for each pH considered (Table 3). It can be seen that increasing pH lead to a decrease of the drug stability, while CBR improved the aqueous stability of PIL for the two pHs studied. The stabilizing effects at pHs 7.0 and 8.0, calculated as the ratio of the rate constants  $k_{\text{obs}}(\text{complex})/k_{\text{obs}}(\text{free})$ , were 3.3 and 3.5, respectively (where  $k_{\text{obs}}(\text{complex})$  and  $k_{\text{obs}}(\text{free})$  represent the rate constants in the presence or absence of the polymer, respectively).

In addition, the thermal effect on PIL degradation, with and without CBR, was studied in the temperature range from 40 to 70 °C, at pH 7.0. Fig. 3 shows the Arrhenius plot of the rate constant ( $\log k_{\text{obs}}$ )

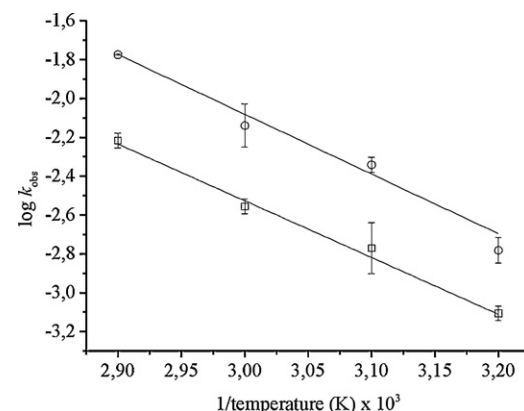


Fig. 3. Arrhenius plot of PIL in free (□) and complex (○) form.

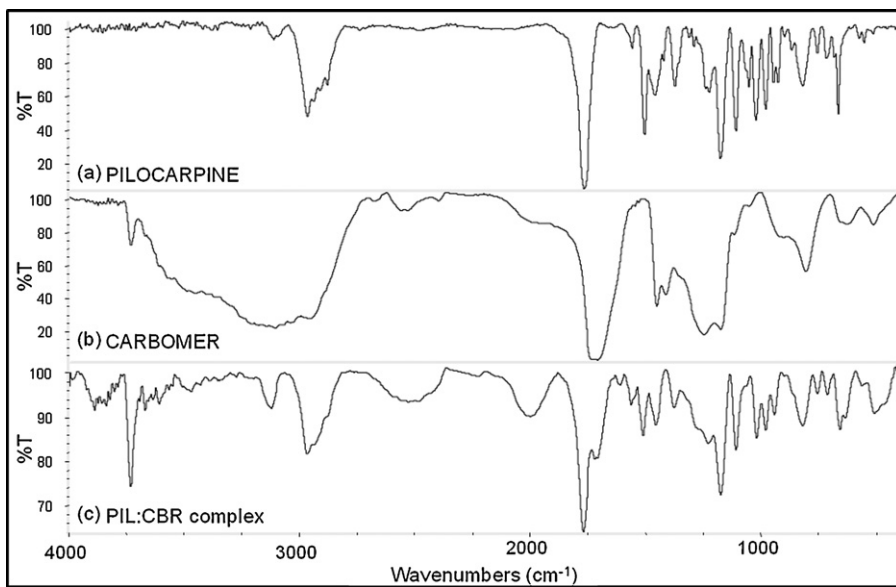


Fig. 4. FT-IR spectra of (a) pure PIL, (b) pure CBR, (c) PIL:CBR complex prepared by freeze-drying.

**Table 4**

Values of  $E_a$ ,  $\log A$ , of PIL in the free and complex.

System	$E_a$ (kcal mol <sup>-1</sup> )	$\log A$
PIL free	14.8 ± 0.5	7.6 ± 0.3
Complex PIL:CBR	13.9 ± 0.4	6.1 ± 0.3

scale) versus the reciprocal of absolute temperature, given by Eq. (3):

$$\log k_{\text{obs}} = \log A - \frac{E_a}{2.303RT} \quad (3)$$

where  $k_{\text{obs}}$  is the pseudo-first order rate constant,  $A$  is the frequency factor,  $E_a$  is the energy of activation of the reaction,  $R$  is the gas constant, and  $T$  is the absolute temperature. A linear relationship was found from these plots (with regression coefficients  $r=0.992$

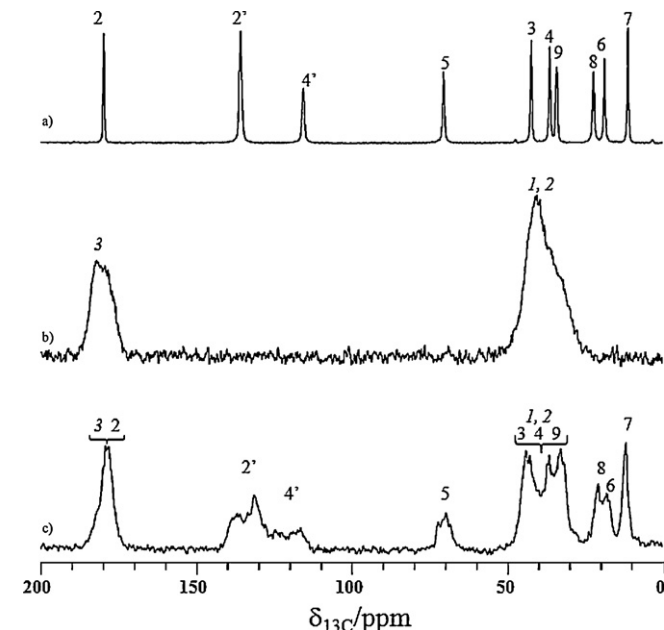


Fig. 5. Solid state  $^{13}\text{C}$  CP/MAS NMR spectra of (a) pure PILCH, (b) pure CBR, (c) PIL:CBR complex prepared by freeze-drying.

and 0.982, with and without CBR, respectively). The values for the activation energy and  $\log A$  are presented in Table 4. An important aspect is that the stabilization of PIL has its origin in a decrease in the effective number of collisions that occurred between molecules in the dispersion, which led to a reduced reactivity for PIL. Note that these results may be correlated with the decrease in the diffusion coefficient observed for PIL obtained using the DOSY technique ( $D$  ( $\text{m}^2/\text{s} \times 10^{10}$ ))  $7.5 \pm 0.03$  and  $4.20 \pm 0.03$  for the free drug and complex, respectively). Moreover, since the PIL:CBR system exhibits a negative electrokinetic potential ( $-42.8 \pm 0.4$  mV) that attracts positive ions such as ( $\text{H}^+$ ) and repels negative ones such as ( $\text{OH}^-$ ), the stabilizing effect could be associated with the higher acidity of the (PIL:CBR) environment (Jimenez-Kairuz et al., 2004).

### 3.3. Complex formation in solid state

In order to test for possible intermolecular interactions between PIL and CBR in the solid state, FT-IR, SSNMR, X-ray powder diffraction, SEM, DSC and TGA were applied.

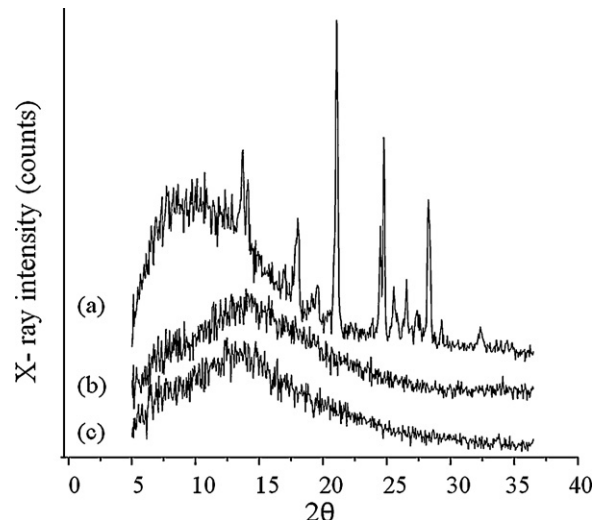
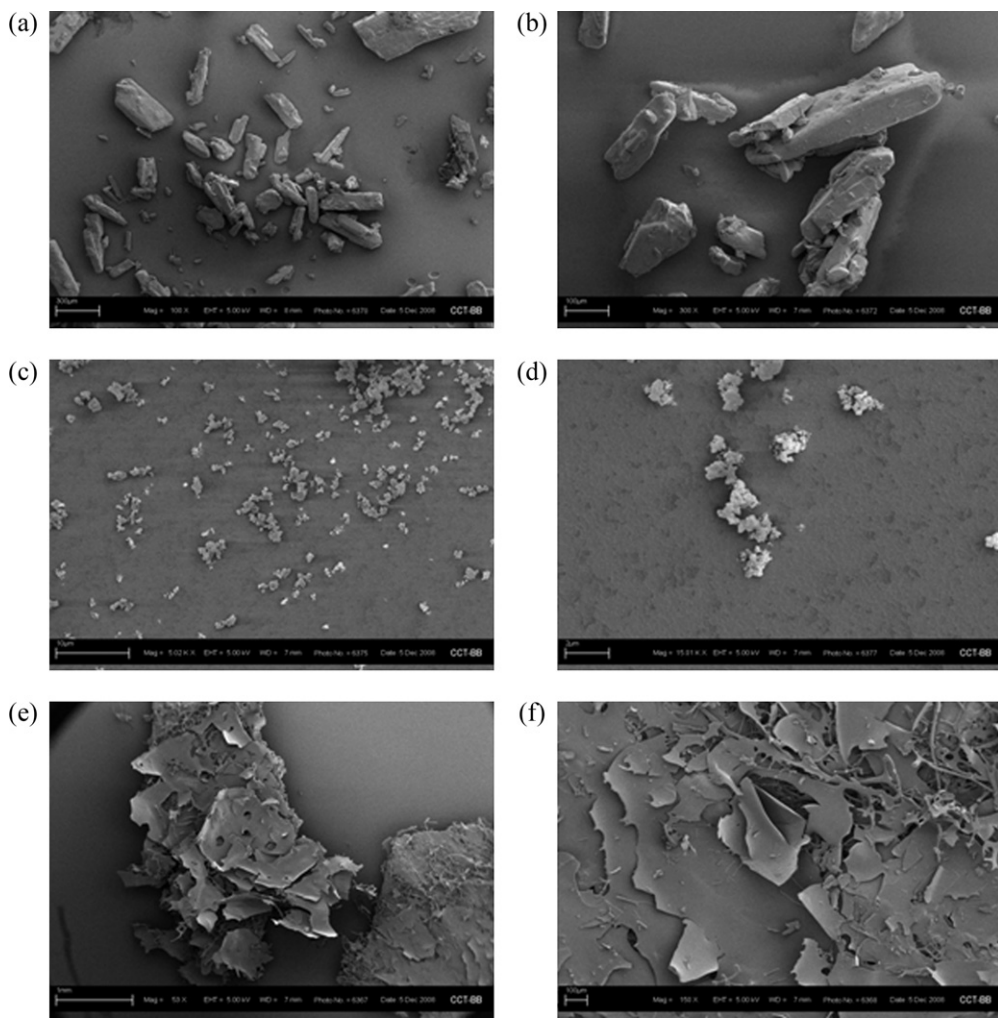


Fig. 6. X-ray diffractograms (a) pure PILCH, (b) pure CBR, (c) PIL:CBR complex prepared by freeze-drying.



**Fig. 7.** Scanning electron microphotographs (a and b) pure PILCH, (c and d) pure CBR, (e and f) PIL:CBR complex prepared by freeze-drying.

### 3.3.1. FT-IR studies

When a drug and a polyelectrolyte form a complex, the FT-IR spectra reveal considerable differences in comparison with the pure components. Specifically, the interactions can shift or change the band intensities and broaden the corresponding vibrations of the raw materials.

The FT-IR spectra of pure components and complex are shown in Fig. 4, where it can be observed that the FT-IR spectrum of PIL contains some characteristic bands at 3160 and 2800  $\text{cm}^{-1}$  due to absorption of the  $-\text{CH}$ ,  $-\text{CH}_2$  and  $-\text{CH}_3$  groups, and at 1770  $\text{cm}^{-1}$  corresponding to the carbonyl group of the lactone ring. In the CBR spectrum, the broad and intense band (between 3460 and 3060  $\text{cm}^{-1}$ ) corresponds to the free hydroxyl group and the hydroxyl-forming intramolecular hydrogen bonding. In addition, at about 1718  $\text{cm}^{-1}$ , there is a  $\text{C}=\text{O}$  stretching band due to the numerous carboxylic acids present in the polymer.

The FT-IR spectrum of the binary system PIL:CBR shows strong, broad N–H stretching absorptions in the 1900–2100  $\text{cm}^{-1}$  region, which are not observed in the raw materials. Moreover, the strong reduction of the characteristic  $\text{C}=\text{O}$  stretching band of the CBR can be seen at 1718  $\text{cm}^{-1}$ . These differences in the FT-IR spectrum of the complex are a result of the electrostatic interaction between the tertiary amine groups of PIL and the carboxyl groups of CBR during complex formation.

### 3.3.2. Solid state nuclear magnetic resonance studies

Further information about the interaction between the different groups of PIL and CBR was obtained by performing SSNMR studies, due to the fact that formation of the complex may change the conformation and the electromagnetic environment of both the drug and the polymer molecules, which would be demonstrated by changes in chemical shift and/or line shape.

In Fig. 5a, the  $^{13}\text{C}$  CP MAS spectrum obtained for pure PIL can be observed [Considering that PIL base cannot be used in these assays due to its melting at room temperature, PIL hydrochloride (PILCH) was used instead]. The  $^{13}\text{C}$  signal assignments (see carbon numbering in Fig. 1a) were achieved based on aqueous NMR spectroscopic data for PIL. In the spectrum of pure PILCH, the following resonance occurred: C2 (180 ppm), C4' and C2' (135 and 115 ppm, respectively), C5, C3 and C4 (70, 42 and 37 ppm, respectively), C9 (33 ppm), and C8, C6 and C7 (22, 18 and 10 ppm, respectively). The resonance lines of pure CBR appeared at around 22–50 ppm (backbone methine and methylene) and between 170 and 190 ppm (carbonyl carbon) (Fig. 5b, see carbon numbering in Fig. 1e).

For the PIL:CBR system, broad lines are observed in the  $^{13}\text{C}$  CP MAS NMR spectrum (Fig. 5c), indicating that the solid complex obtained by freeze-drying may be amorphous. Significant changes in the resonances corresponding to PIL and CBR occurred upon complexation. Major modifications were found for the C4' and C2' drug

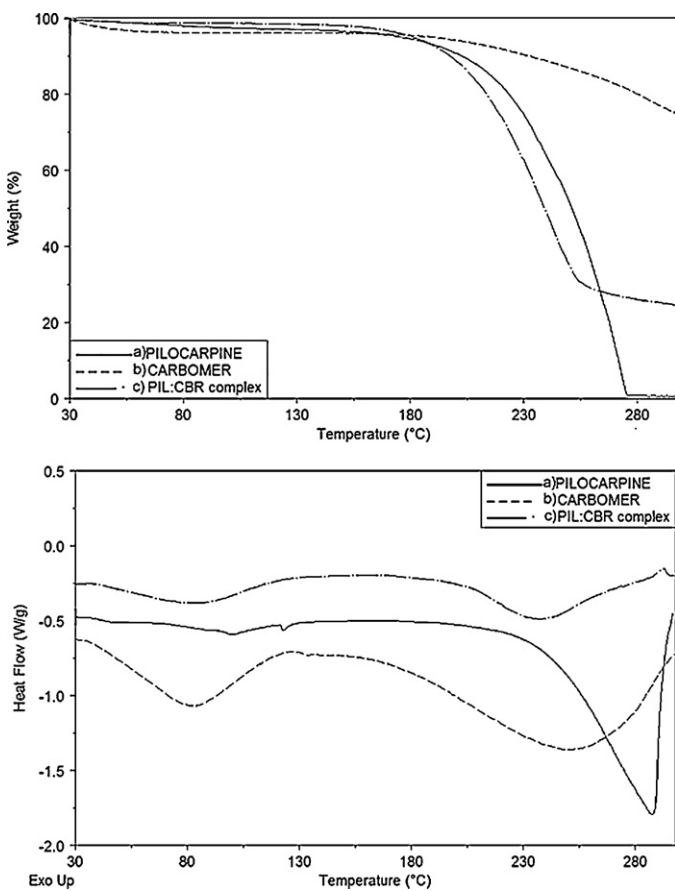


**Fig. 8.** DSC and TG curves of (a) PIL, (b) CBR, (c) PIL:CBR complex prepared by freeze-drying.

nuclei and the C3 polymer nuclei, thus confirming the presence of electrostatic interactions between PIL and CBR.

### 3.3.3. X-ray powder diffraction studies

In order to determine the degree of crystallinity of the PIL:CBR complex prepared by freeze-drying, diffractograms of raw materials and the complex were recorded, with the diffraction patterns obtained being shown in Fig. 6.

The diffraction pattern of PILCH (Fig. 6a) shows the presence of peaks at the following diffraction angles ( $2\theta$ ):  $13.7^\circ$ ,  $18^\circ$ ,  $21.1^\circ$ ,  $24.8^\circ$ ,  $25.5^\circ$ ,  $25.6^\circ$  and  $32.2^\circ$ , indicating that the drug was present in the crystalline form, while the absence of diffraction peaks in the X-ray diffraction patterns of the polymer and the PIL:CBR complex is indicative of the amorphous nature of both samples (Fig. 6b and c).

### 3.3.4. Scanning electron microscopy studies

Scanning electron microscopy was used to study the microscopic appearance of the compounds and to evaluate the morphology of the PIL:CBR complex.

For the reasons mentioned above, the microphotographs observed in Fig. 7a and b correspond to PILCH. This drug is present in the form of crystalline particles of irregular shape and size. In contrast, the microphotographs obtained for the pure polyelectrolyte (Fig. 7c and d) show the presence of amorphous, small and homogeneous particles.

In the freeze-dried product, the original morphology of the raw materials was not present, and it was not possible to differentiate between the two components (Fig. 7e and f), with the sample

appearing as an amorphous solid. This drastic change in the particle shape and aspect may indicate the presence of a new solid phase.

### 3.3.5. DSC and TGA studies

The DSC and TGA curves of pure PIL and CBR along with the corresponding complex prepared by freeze-drying are shown in Fig. 8.

The DSC curve of pure PIL shows an endothermic event at temperatures above  $180^\circ\text{C}$ , which may be attributed to drug decomposition based on the results obtained from the TG curve (96.3% mass loss). In the curves obtained for pure CBR, two endothermic processes can be observed. The first one between 50 and  $100^\circ\text{C}$  is due to the removal of the residual solvent (3.5% mass loss), and the second at temperatures above  $200^\circ\text{C}$  occurred because of the decomposition of the product. At approximately  $125^\circ\text{C}$ , a small change in the baseline of the DSC curve of CBR can be seen, caused by the glass transition of the macromolecule. In the curves obtained for the sample prepared by freeze-drying, it can be observed that the decomposition begins at  $180^\circ\text{C}$  (73.7% mass loss).

## 4. Conclusions

The interaction between PIL and CBR in solution and in solid state was confirmed, with this being favored by the electrostatic interactions between the amine group of the drug and the carboxylic acid group of CBR. Furthermore, this interaction was demonstrated to have a positive effect on drug stability. From the Arrhenius plots, it could be concluded that the observed stabilizing effect on PIL is due to a decrease in the effective number of collisions that occurred between the molecules present in the dispersion. This is important, because it might indicate that to observe a stabilizing effect on a particular drug, a specific conformation of the drug: polyelectrolyte complex is not required, because while interactions take place, the reaction rate may be decreased as a result of reduced mobility of the drug molecules.

In addition, from the results obtained in solid state, the formation of a complex between PIL and CBR was achieved by applying a freeze-drying method, which might be of use at an industrial scale. Taking into account that the currently available treatments of xerostomia are of short duration, the PIL:CBR system provides an interesting alternative for the preparation of extended release matrices of PIL, which may allow a reduction in the frequency of administration.

## Acknowledgments

This work was supported by Fondo para la Investigación Científica y Tecnológica (FONCYT) Préstamo BID PICT 1376, the Secretaría de Ciencia y Técnica de la Universidad Nacional de Córdoba (SECyT), the Consejo Nacional de Investigaciones Científicas y Tecnológicas de la Nación (CONICET) and the Ministerio de Ciencia y Tecnología de la Provincia de Córdoba. We are grateful to Dr. Gloria M. Bonetto for NMR measurements and for her helpful discussion of the  $^1\text{H}$  NMR spectra. The authors also thank Laboratorios Beta for their donation of pilocarpine hydrochloride.

## References

- Al-Badr, A.A., Aboul-Enein, H.Y., 1983. Pilocarpine. In: Florey, K. (Ed.), *Analytical Profiles of Drug Substances*. Academic Press, New York, pp. 385–428.
- Bennet, A.E., Rienstra, C.M., Auger, M., Lakshmi, K.V., Griffin, R.G., 1995. Heteronuclear decoupling in rotating solids. *J. Chem. Phys.* 103, 6951–6958.
- Bundgaard, H., Hansen, S.H., 1982. Hydrolysis and epimerization kinetics of pilocarpine in basic aqueous solution as determined by HPLC. *Int. J. Pharm.* 10, 281–289.

Clinical Pharmacology Online, 2009. Gold Standard, an Elsevier Company, Tampa, FL. Available from URL: [www.clinicalpharmacology.com](http://www.clinicalpharmacology.com). Cited November 18, 2010.

Connors, K.A., Amidon, G.L., Stella, V.J., 1986. Pilocarpine. In: Chemical Stability of Pharmaceuticals, 2nd ed. John Wiley & Sons, New York, pp. 675–684.

Esteban, S.L., Manzo, R.H., Alovero, F.L., 2009. Azithromycin loaded on hydrogels of carbomer: chemical stability and delivery properties. *Int. J. Pharm.* 366, 53–57.

Harris, R.K., 1994. Nuclear Magnetic Resonance Spectroscopy. Longman Scientific and Technical, London.

Huo, R., Wehrens, R., van Duynhoven, J., Buydens, L.M.C., 2003. Assessment of techniques for DOSY NMR data processing. *Anal. Chim. Acta* 490, 231–251.

International Conference on Harmonization (ICH) of Technical Requirements for registration of Pharmaceuticals for Human Use, Topic Q1A(R2): Stability testing of new drug substances and products, Geneva, 2003.

International Conference on Harmonization (ICH) of Technical Requirements for registration of Pharmaceuticals for Human Use, Topic Q2(R1): Validation of analytical procedures: text and methodology, Geneva, 2005.

Jarvinen, K., Jarvinen, T., Thompson, D.O., Stella, V.J., 1994. The effect of a modified  $\beta$ -cyclodextrin, SBE4- $\beta$ -CD, on the aqueous stability and ocular absorption of pilocarpine. *Curr. Eye Res.* 13, 897–905.

Jimenez-Kairuz, A., Allemandi, D., Manzo, R.H., 2002. Mechanism of lidocaine release from carbomer-lidocaine hydrogels. *J. Pharm. Sci.* 91, 267–272.

Jimenez-Kairuz, A.F., Allemandi, D.A., Manzo, R.H., 2003. Equilibrium properties and mechanism of kinetic release of metoclopramide from carbomer hydrogels. *Int. J. Pharm.* 250, 129–136.

Jimenez-Kairuz, A.F., Allemandi, D.A., Manzo, R.H., 2004. The improvement of aqueous chemical stability of a model basic drug by ion pairing with acid groups of polyelectrolytes. *Int. J. Pharm.* 269, 149–156.

Jimenez-Kairuz, A.F., Llabot, J.M., Allemandi, D.A., Manzo, R.H., 2005. Swellable drug-polyelectrolyte matrices (SDPM): characterization and delivery properties. *Int. J. Pharm.* 288, 87–99.

Sweetman, S.C., Blake, P.S., 2009. Martindale: The Complete Drug Reference, 36 ed. Pharmaceutical Press, London.

Vilches, A.P., Jimenez-Kairuz, A.F., Alovero, F.L., Olivera, M.E., Allemandi, D.A., Manzo, R.H., 2002. Release kinetics and up-take studies of model fluoroquinolones from carbomer hydrogels. *Int. J. Pharm.* 246, 17–24.

Wong, O., Anderson, C., Allaben, L., Pabmanabhan, R., Lattin, G., 1991. Stability-indicating assay method for pilocarpine nitrate in reservoirs used in the cystic fibrosis indicator system. *Int. J. Pharm.* 76, 171–175.

Yoshioka, S., Stella, V., 2002. Chemical stability of drug substances. In: Stability of Drugs and Solid Dosage Forms. Kluwer Academic Publishers, USA, pp. 3–137.